4-22-2021

Mobile Protons Limit the Stability of Salt Bridges in the Gas Phase: Implications for the Structures of Electrosprayed Protein Ions.

Lars Konermann

Elnaz Aliyari

Justin H Lee

Mobile Protons Limit the Stability of Salt Bridges in the Gas Phase: Implications for the Structures of Electrosprayed Protein Ions

Lars Konermann* Elnaz Aliyari, and Justin H. Lee

Department of Chemistry, The University of Western Ontario, London, Ontario, N6A 5B7, Canada.

* corresponding author

E-mail address of the corresponding author: konerman@uwo.ca

Funding was provided by the Natural Sciences and Engineering Research Council of Canada (RGPIN-2018-04243).

ABSTRACT: Electrosprayed protein ions can retain native-like conformations. The intramolecular contacts that stabilize these compact gas phase structures remain poorly understood. Recent work has uncovered abundant salt bridges in electrosprayed proteins. Salt bridges are zwitterionic BH^+/A^- contacts. The low dielectric constant in the vacuum strengthens electrostatic interactions, suggesting that salt bridges could be a key contributor to the retention of compact protein structures. A problem with this assertion is that H^+ are mobile, such that H^+ transfer can convert salt bridges into neutral B^0/HA^0 contacts. This possible salt bridge annihilation puts into question the role of zwitterionic motifs in the gas phase, and it calls for a detailed analysis of BH^+/A^- vs. B^0/HA^0 interactions. Here we investigate this issue using molecular dynamics (MD) simulations and electrospray experiments. MD data for short model peptides revealed that salt bridges with static H^+ have dissociation energies around 700 kJ mol^{-1}. The corresponding B^0/HA^0 contacts are one order of magnitude weaker. When considering the effects of mobile H^+, BH^+/A^- bond energies were found to be between these two extremes, confirming that H^+ migration can significantly weaken salt bridges. Next, we examined the protein ubiquitin under collision-induced unfolding (CIU) conditions. CIU simulations were conducted using three different MD models: (i) Positive-only runs with static H^+ did not allow for salt bridge formation and produced highly expanded CIU structures. (ii) Zwitterionic runs with static H^+ resulted in abundant salt bridges, culminating in much more compact CIU structures. (iii) Mobile H^+ simulations allowed for the dynamic formation/annihilation of salt bridges, generating CIU structures intermediate between scenarios (i) and (ii). Our results uncover that mobile H^+ limit the stabilizing effects of salt bridges in the gas phase. Failure to consider the effects of mobile H^+ in MD simulations will result in unrealistic outcomes under CIU conditions.

Introduction

In aqueous solution, most proteins spontaneously fold into compact structures.[1] Deciphering the interplay of stabilizing and destabilizing factors that shape these native conformations remains a formidable challenge.[2-4] A major contributor to the stability of the native state in solution is the clustering of hydrophobic residues in the core, reflecting the tendency of nonpolar side chains to avoid water.[1, 5] Native proteins are also stabilized by H-bonds and van der Waals interactions. Another factor that is often mentioned in this context is the formation of salt bridges.[6]

A salt bridge is a zwitterionic contact between a protonated basic site (BH^+) and a deprotonated acidic site (A^-). BH^+ can be Arg^+, Lys^+, His^+, or the N-terminus (NT^+), while A^- can be a carboxylate of Glu^-, Asp^-, or the C-terminus (CT^-). In addition to electrostatic attraction, each salt bridge involves at least one H-bond.[7, 8] Crystallography has shown that most salt bridges are on the protein surface.[9] The role of these contacts for proteins in solution remains unclear. Salt bridge formation requires partial desolvation of BH^+ and A^-, a process that is energetically unfavorable.[8, 10] Also, attractive positive/negative interactions are weakened by the high dielectric constant of water, and by dissolved salts that cause Debye-Hückel screening.[9, 11] As a result, the stabilizing effects of salt bridges in solution are likely very small.[8-11]

Electrospray ionization (ESI)[12] generates gaseous biomolecular ions, creating opportunities for protein stability studies complementary to those in solution. $[M + zH]^{z+}$ protein ions produced by "native" ESI can maintain solution-like conformations.[13-21] This structural robustness has been attributed to kinetic trapping, i.e., the presence of large activation barriers that preclude transitions to thermodynamically stable gas phase structures.[19, 22-25] Many aspects of gaseous proteins remain poorly understood,[19, 26, 27] largely because mass spectrometry (MS) and ion mobility spectrometry (IMS) experiments only provide low-resolution structural insights. Molecular dynamics (MD) simulations have therefore become an important tool in this area.[24, 26, 28-34]

Solvent removal during ESI has profound implications for intramolecular contacts. The lack of water implies a substantial weakening of the hydrophobic effect.[24, 35-38] The change in dielectric constant from water ($\varepsilon \approx 80$) to vacuum ($\varepsilon = 1$) strengthens electrostatic interactions, keeping in mind the $1/\varepsilon$ dependence in Coulomb's Law.[5, 39, 40] Thus, salt bridges should be much more stable in vacuum than in water.[5, 39] Some studies even suggest that gas phase salt bridges can be more stable than covalent bonds.[40, 41] Despite this seemingly straightforward assertion, the role of salt bridges in the gas phase is yet to be fully explored.

As a starting point, one has to ask if salt bridges can even exist in the gas phase. Early studies suggested that the high proton affinity (*PA*) of carboxylates will annihilate salt bridges via H^+ transfer, thereby generating charge-neutralized motifs.[42, 43]

$$BH^+/A^- \quad \underset{\leftarrow}{\overset{\rightarrow}{}} \quad B^0/HA^0 \qquad (1)$$

Accordingly, many gas phase MD studies on $[M + zH]^{z+}$ ions have been conducted in "positive-only" mode, i.e., by allowing for exactly z BH^+ sites without any A^-.[28, 29, 32, 44] However, recent experimental and computational work has uncovered that zwitterionic motifs including salt bridges can be highly abundant in electrosprayed biomolecular ions.[30, 31, 45-50]

A back-of-the-envelope calculation[51] qualitatively illustrates under what conditions a salt bridge can exist in the gas phase (Figure 1A). When treating BH^+ and A^- as point charges, and when neglecting entropy effects ($T|\Delta S| << |\Delta H|$),[42] the free energy of reaction 1 can be expressed as

$$\Delta G = \mathrm{PA(B)} - \mathrm{PA(A^-)} + \frac{e^2}{4\pi\varepsilon_0 r} \qquad (2)$$

Figure 1 displays ΔG as a function of distance r between the two point charges, using *PA* values of Lys and Asp^-. The zwitterionic state Lys^+/Asp^- is favored when the distance is small ($\Delta G > 0$ for r

< 0.26 nm), as ΔG is dominated by the electrostatic attraction between the two charges. For larger distances the electrostatic attraction diminishes, favoring charge-neutralized Lys^0/Asp^0 ($\Delta G < 0$ for $r > 0.26$ nm). Such H^+ transfer is in line with QM/MM data,[52] reflecting the mobile nature of H^+ in gaseous proteins.[52-56] Similarly, salt-bridged Ser_8^+ clusters release Ser^0 moieties upon collisional activation, suggesting that dissociation is concomitant with salt bridge neutralization.[57] Numerous studies[45-49] support the prediction of Figure 1B that gas phase salt bridges exist only for base/acid sites that are in close proximity to one another. Figure 1C plots the distance dependence of the Lys^+/Asp^- potential energy ($V(r) = -PA(Lys) - e^2/4\pi\varepsilon_0$), as well as $V(r) = -PA(Asp^-)$ for the Lys^0/Asp^0 neutralized form. As r increases, H^+ transfer causes a crossover from the former to the latter $V(r)$ profile, generating an effective $V(r)$ that is indicated by the magenta dots in Figure 1C.

To be clear, the simple model of eq. 2 (Figure 1) was introduced only to highlight the problem in a qualitative fashion. For predicting the protonation state of a base/acid pair more accurately, one has to consider charge solvation[47, 55, 58-60] and H-bonding between the base/acid moieties.[7, 8] The MD data discussed below take into account all of these details, as well as Lennard-Jones interactions among the participating atoms (see below).[60]

The preceding considerations highlight an interesting conundrum. On the one hand, salt bridges are expected to be very strong in a low dielectric vacuum environment.[5, 39, 40] They should therefore help preserve compact conformations in the gas phase.[30, 45, 47] On the other hand, salt bridges appear to be fragile because they can undergo annihilation via H^+ transfer - although the neutralized B^0/HA^0 may still stabilize the protein to some extent by retaining H-bonding.[30] Thus, much remains to be learned regarding the role of salt-bridged vs. neutral base/acid contacts in the gas phase.

The stability of gaseous proteins can be probed by exposing them to collisional heating.[21, 49, 61-66] Collisions with background gas gradually raise the internal energy and trigger collision-induced

unfolding (CIU) which can be probed by IMS.[28, 65-68] Here we explore the effects of salt bridges on the CIU behavior of ubiquitin, a commonly used model protein.[19, 30, 31, 45, 67, 69, 70] Ubiquitin ions generated by native ESI possess a number of salt bridges,[30, 45] making them suitable for examining the role of BH^+/A^- vs. B^0/HA^0 contacts. We combine experiments and simulations, with emphasis on a mobile H^+ MD technique[30, 60] that captures the capability of H^+ to migrate in gaseous proteins,[52-56] allowing for the formation/annihilation of salt bridges (eq. 1). This method overcomes a key limitation of traditional MD simulations, where protonation patterns remain static throughout the entire run.[24, 26, 28, 29, 31, 33, 34] We find that, despite the fleeting nature of charge-charge contacts, salt bridges promote the preservation of compact structures during CIU. However, this stabilization is less pronounced than might be expected from zwitterionic models that neglect the mobile nature of H^+.

Methods

ESI-MS and IMS. Native ESI experiments were performed on a Synapt G2Si time-of-flight mass spectrometer (Waters, Milford, MA). Bovine ubiquitin (8565 Da, Sigma, St. Louis, MO) was electrosprayed at +2.8 kV using a standard Z-spray ESI source at 5 µL min^{-1} in 10 mM aqueous ammonium acetate solution (pH 7) under gentle ion sampling conditions (source temperature 25 °C, desolvation temperature 40 °C, sampling cone 5 V). Collisional heating was implemented in the trap cell with Ar as collision gas. Following quadrupole selection of 6+ ions, the trap collision energy was adjusted to values between zero and 80 V. Collision cross sections (Ω) were measured in N_2 buffer gas by traveling wave IMS, and a calibration procedure was employed for converting arrival time distributions to He Ω values.[71]

Protein Molecular Dynamics Simulations. Vacuum MD simulations on ubiquitin were performed using Gromacs 2016 with GPU acceleration,[72] with the X-ray coordinates 1UBQ as starting point. Bond distances were constrained, and the integration step was 1 fs. Runs were conducted without cutoffs for Lennard Jones or Coulomb interactions.[30] Side chain protonation patterns were controlled using the Gromacs pdb2gmx module. The simulations employed the OPLS-AA/L force field[73] which has been widely used for earlier MD studies on gaseous protein ions including ubiquitin.[30, 45, 74-76] Also, OPLS-AA/L has been validated against *ab initio* gas phase data.[73] The protein was equilibrated at 300 K for 30 ns, followed by 100 ns of heating at a rate of 7 K ns^{-1} for a final temperature of 1000 K. Similar to earlier simulations,[32] the background gas surrounding the protein during CIU was not modeled explicitly. This strategy reflects the fact that structural changes experienced by protein ions are indistinguishable for different slow heating methods, e.g., gas collisions or exposure to blackbody infrared radiation.[56] The temperature was controlled using the Nosé-Hoover algorithm[77] which resulted in more stable runs at high temperature than other thermostats. All runs were repeated five times with different initial velocities that were sampled at random from a Maxwell-Boltzmann distribution at the desired temperature.

Mobile H^+ simulations were conducted as described[30, 60] by complementing Gromacs with in-house Fortran code and bash scripts. MD runs were dissected into 142 ps segments. After each segment the H^+ residing on all protonated sites (NT^+, Arg^+, Lys^+, His^+, Asp^0, Glu^0, CT^0) were redistributed using an energy minimization procedure that takes into account the *PA* of all possible acceptor sites. The following *PA* values in kJ mol^{-1} were used: 886.6 (NT), 918.0 (Lys), 1002.0 (Arg), 952.7 (His), 1452.7 (Asp^-), 1453.5 (Glu^-), 1450.0 (CT^-).[42] In addition, energy minimization considered the electrostatic contributions from all atoms. In this way we accounted for intramolecular charge solvation, as well as H-bonding (OPLS-AA/L treats H-bonds as electrostatic

contacts, with hydrogen Lennard-Jones ε and σ values of zero).[78] Ideally, the mobile H^+ simulations would involve QM/MM,[52, 79, 80] *ab initio* MD[81-84] or DFT/MD methods.[85] However, the computational cost of those methods precludes their application to large systems such as proteins, particularly for simulations on long time scales (hundreds of nanoseconds). In contrast, the mobile H^+ method used here can readily be used for large systems and long simulation windows. Despite the conceptual simplicity of our mobile H^+ method it has proven to robust, yielding results that are consistent with experimental observations. Examples include the formation of salt bridge networks on the surface of protein ions generated by native ESI,[30] and the ejection of highly charged monomers from collisionally heated complexes.[51]

Neutral His was modeled as Nε2-H tautomer (HisE), which dominates over the HisD form in peptides and proteins.[86] He collision cross sections of MD structures were calculated using the trajectory method in Collidoscope[87] at 300 K (prior to equilibration), 300 K (after equilibration), 475 K, 650 K, 825 K, and 1000 K.

Peptide Pulling Simulations. Center of mass (COM) pulling simulations (also known as steered MD[88-90]) were conducted on small model peptides in vacuum at 300 K. These MD runs used existing Gromacs tools[91] with static protonation patterns and neutral peptide termini. Peptide 1 contained a basic residue and peptide 2 contained Glu. Charged and neutral side chains were tested. The initial peptide conformations were excised from a ubiquitin MD structure surrounding salt-bridged Lys11 and Glu34. To simplify the simulations both Thr12 and Lys33 were changed to Ala, yielding Gly-Lys-Ala (peptide 1) and Ala-Glu-Gly (peptide 2). For simulations involving other peptide 1 versions, Lys → Arg or Lys → His substitutions were performed using Pymol. Following energy minimization, the peptides were equilibrated for 100 ps at 300 K while restraining heavy atoms (excluding the basic/acidic side chains) in a 3D harmonic potential with a force constant of 1000 kJ

mol^{-1} nm^{-2}. This equilibration ensured relaxed side chain contacts (salt bridges and/or H-bonds) prior to pulling. A force F was then applied to the peptide 1 COM, such that peptide 1 was pulled away from peptide 2 in positive y direction, while the aforementioned position restraints were retained for peptide 2. F did not act on the side chains of Lys, Arg, His and Glu. The COM harmonic pulling force constant was K_{pull} = 1000 kJ mol^{-1} nm^{-2} and the pulling speed was v_{pull} = 0.001 nm ps^{-1}. Preliminary tests (not shown) revealed that simulations with five times higher v_{pull} generated $F(t)$ profiles that were virtually identical to those discussed below. All pulling runs were repeated five times with different equilibrated starting structures.

Results and Discussion

Prior to studying the role of salt bridges during protein CIU, it is instructive to examine small model systems. For this purpose we performed gas phase MD simulations on peptides that were linked by a BH^+/A^- salt bridge or by a B^0/HA^0 contact. COM pulling[91] was applied to assess the peptide interaction strength. Peptide 1 was attached to a virtual spring while peptide 2 was held in place. Pulling on the spring with constant velocity exerted a gradually increasing force $F(t)$ on peptide 1, culminating in rupture of the peptide-peptide contacts. We performed these pulling simulations under traditional MD conditions,[24, 26, 28, 29, 31, 33, 34] where H^+ were *not* allowed to transfer from one site to another. Subsequently we explored how the outcome of these simulations would change when allowing for H^+ transfer.

Pulling Data for Salt-Bridged Gas Phase Peptides. Figure 2A depicts the salt-bridged peptides Gly-Lys^+-Ala (peptide 1) and Ala-Glu^--Gly (peptide 2). The direction of the force $F(t)$ acting on peptide 1 is indicated. Rupture of the Lys-NH_3^+/$^-$OOC-Glu salt bridge occurred at $t \approx 2096$ ps. $F(t)$

showed a near-linear increase (Figure 2B). Consistent with earlier COM pulling studies,[91] this $F(t)$ behavior is dominated by the harmonic nature of the pulling force (Hooke's Law: $|F(t)| = K_{pull} \times v_{pull} \times t$), rather than the Coulomb forces, H-bonds, and Lennard-Jones contacts that connect the two peptides. The distance between the closest Lys^+/Glu^- atoms remained almost constant up until the dissociation event (Figure 2C). Dissociation is marked by a sudden distance increase (Figure 2C) that coincides with a force drop-off (Figure 2B). The triangular $F(t)$ profiles in Figure 2B are reminiscent of mechanical protein unfolding experiments which also involve the dissociation of noncovalent contacts.[90]

The $F(t)$ profiles show some deviations from linearity for early simulation times (up to ~ 700 ps, Figure 2B). These nonlinearities arise from the rupture of secondary H-bonds that had formed during equilibration (between NT^0 of peptide 1 and Glu^- of peptide 2, and between Lys^+ and a backbone CO of peptide 2 (Figure 2A, 1 ps). These secondary contacts dissociated long before rupture of the Lys^+/Glu^- salt bridge. For example, at t = 1200 ps the secondary H-bonds had disappeared while the salt bridge persisted (Figure 2A).

Pulling Data for Neutral Gas Phase Peptides. Pulling simulations were repeated under conditions where the two peptides interacted through a Lys^0/Glu^0 contact (Figure 2D-F). The two neutral side chains initially formed a H-bond, either Lys-NH···OC-Glu or Lys-N···HO-Glu. In addition, some starting structures had a secondary H-bond between Lys-NH and a backbone CO of peptide 2 (Figure 2D, 1 ps). Pulling quickly ruptured this secondary contact, generating a scenario where the side chains were H-bonded via Lys-N···HO-Glu for all runs (Figure 2D, 660 ps). Subsequently, these Lys^0/Glu^0 contact dissociated (Figure 2D, 794 ps). This Lys^0/Glu^0 dissociation took place much earlier (830 ± 60 ps, Figure 2F) than for the Lys^+/Glu^- scenario (2010 ± 60 ps, Figure 2C).

Dissociation Energies of Salt-Bridged vs. Neutral Contacts. For quantifying the interaction strength associated with the Lys^+/Glu^- and Lys^0/Glu^0 scenarios of Figure 2 we determined peptide-peptide dissociation energies (*DE*) according to

$$DE = \int_0^{3000\ ps} F(t)\ v_{pull}\ dt \qquad (3)$$

In this equation, $F(t)$ is the pulling force as a function of time (Figure 2B/E), and v_{pull} = 0.001 nm ps^{-1} is the pulling velocity. *DE* values obtained in this way are (1070 ± 10) kJ mol^{-1} for the salt-bridged system, and (86 ± 4) kJ mol^{-1} for the neutral peptides. These dramatically different *DE*s are in line with the expectation that salt bridges in the gas phase are very stable.[39, 40] However, a detailed understanding of base/acid contacts requires us to consider two additional issues.

(1) The *DE* values calculated from eq. 3 include contributions from Lys/Glu contacts as well as secondary H-bonds (explained above). The latter can be excluded using a linear extrapolation strategy (Figure S1). This procedure yields corrected *DE* values that exclusively reflect the Lys^+/Glu^- or Lys^0/Glu^0 contacts, (880 ± 10) kJ mol^{-1} and (40 ± 10) kJ mol^{-1}, respectively.

(2) The MD runs of Figure 2A-C assume that the zwitterionic state will persist in perpetuity, ignoring the possibility that the salt bridge may undergo neutralization via H^+ transfer (eq 1, Figure 1).[47, 53-55, 58-60] $Lys^+/Glu^- \rightarrow Lys^0/Glu^0$ conversion would prematurely terminate the $F(t)$ profiles of Figure 2B. Unfortunately, it is difficult to combine mobile H^+ simulations[30, 60] with COM pulling.[91] For assessing the implications of H^+ transfer we applied a "workaround", where coordinates were exported from Lys^+/Glu^- pulling trajectories at various time points. Each of these snapshots was analyzed using the mobile H^+ algorithm to test if the Lys^+/Glu^- state would spontaneously convert to Lys^0/Glu^0. We found that this zwitterionic → neutral conversion becomes favorable for time points later than (1200 ± 200) ps, indicated by the vertical lines in Figure 2B/C. A salt bridge *DE* value that allows for mobile H^+ is thus obtained by integrating eq. 3 between zero and the dashed

lines in Figure 2B, instead of using 3000 ps as the upper bound. After correcting for issues (1) and (2) we found that the Lys^+/Glu^- salt bridge has a *DE* of (200 ± 100) kJ mol^{-1}.

Simulations analogous to the Lys/Glu runs of Figure 2 were conducted for Arg/Glu and His/Glu-linked peptides (Figures S2, S3). The chemical moieties tested in these three types of runs cover all possible base/acid contacts, keeping in mind that the NT has an amine group (akin to Lys) while Asp and the CT are carboxylic acids (akin to Glu). The *DE* values obtained in this way (Table 1) reveal that mobile H^+ reduce the strength of salt bridges by 17% (Arg^+) to 75% (Lys^+). Salt bridges involving Arg^+ are most stable because the high *PA* of Arg[42] tends to retain the mobile H^+ on Arg^+, thereby favoring the preservation of the zwitterionic state. Even after correcting for issues (1) and (2), BH^+/A^- salt bridges were found to be roughly one order of magnitude more stable than the corresponding B^0/HA^0 contacts (Table 1).

Collision-Induced Unfolding Experiments. Native ESI experiments on ubiquitin showed $[ubiquitin + 6H]^{6+}$ to be the most abundant ion (Figure 3A). These 6+ ions were quadrupole-selected and exposed to collisional heating by increasing the trap collision energy (CE). Mass spectra acquired at low CE exclusively showed the covalently intact protein (0 V up to ~50 V, Figure 3B). Higher CE values (50 – 80 V) started to cause collision-induced dissociation (CID), i.e., the rupture of covalent bonds that resulted in *b* and *y* fragments (Figures 3C and S4).[92, 93]

IMS data acquired under the most gentle settings (CE = 0 V, Figure 3D) were dominated by ions with $\Omega \approx 1035$ $Å^2$, corresponding to compact native-like conformers.[19, 30] A less abundant satellite peak at ~1190 $Å^2$ in Figure 3D represents a sub-population that is slightly unfolded.[30] This second species results from heating in the ion sampling interface of the Synapt G2Si instrument. The G2Si utilizes a step-wave ion guide that enhances sensitivity, while being more activating than some other interfaces. When using CE = 0 on a different type of instrument (a Synapt G2) that has

a simple stacked-ring ion guide interface[94] we were able to acquire ESI-IMS data without the ~1190 $Å^2$ species, attesting to more gentle source conditions (Figure S5). These instrument differences are of no concern for the current work, because our focus is on unfolding events.

Exposure of $[ubiquitin + 6H]^{6+}$ to increasing collisional activation caused CIU, evident from shifts to larger Ω in Figure 3D-G. At high CE (80 V, Figure 3G) the mobilogram had its maximum at $\Omega \approx 1490$ $Å^2$ which corresponds to extensively unfolded ubiquitin. Earlier IMS experiments[95] on $[ubiquitin + 6H]^{6+}$ after both solution-phase unfolding and extensive collisional heating yielded 1525 $Å^2$, which is close to the value seen in Figure 3G. Unfortunately, CE values beyond 80 V could not be accessed in our experiments because the ions were destroyed by CID (Figure 3C), and because IMS signal was lost (note that the data in Figure 3G are already very noisy).

The presence of covalent CID products in our experiments (*b* and *y* ions in Figures 3C and S4) reveals that protein heating at *CE* = 80 V is sufficiently harsh to allow the dissociation of bonds with threshold energies of 200-300 kJ mol^{-1}.[96] These energies are on the same order of magnitude as the salt bridge *DE* values determined in this work (last row for each base/acid pair in Table 1). In other words, the occurrence of covalent CID confirms that the rupture of salt bridges during the CIU is energetically feasible – even for salt bridges that have not previously been converted to B^0/HA^0 contacts by transfer of a mobile H^+.

Collision-Induced Unfolding Simulations. It is known from previous work that compact ubiquitin ions at low CE possess a number of salt bridges.[30, 45] How do these BH^+/A^- linkages behave during collisional heating? What would happen if they were replaced with B^0/HA^0 contacts? Do the BH^+/A^- linkages promote the retention of compact conformations, keeping in mind that mobile H^+ can cause salt bridge annihilation (eq. 1)? It is challenging to answer these questions experimentally because one cannot easily alter the protonation behavior of specific side chains. In contrast, MD simulations

allow the properties of titratable sites to be tightly controlled. We therefore conducted vacuum MD runs using three different charge models to examine the CIU behavior of [ubiquitin + 6H]$^{6+}$. Following equilibration at 300 K the ions were heated to 1000 K.

(1) *Positive-only simulations with static H^+* exclusively used BH^+ charges. The lack of A^- implies the absence of salt bridges. H^+ were not allowed to migrate. Such simulations represent the most simplistic type of gas phase protein MD.[29, 97] Five static protonation patterns were tested, all of which had their positive charges distributed over the protein surface. Preference was given to protonation of Arg which has the highest *PA*[42] (Figure S6A). MD runs conducted under these conditions initially retained native-like conformations (Figure 4A) where many of the neutral titratable sites were engaged in B^0/HA^0 H-bonds, along with H-bonds to non-titratable side chain and backbone sites (Figure S7). Heating to 1000 K generated highly extended CIU structures where most of the noncovalent contacts were disrupted (Figure 4A).

(2) *Zwitterionic simulations with static H^+* employed both BH^+ and A^- sites, using the protonation patterns depicted in Figure S6B. MD runs of this type have previously been conducted on a range of proteins.[45, 76, 98] While allowing for the known presence of salt bridges in gaseous proteins,[30, 31, 45-50] this approach still does not permit H^+ migration. Compact ubiquitin conformers early during the MD runs had various salt bridges at the protein surface. CIU structures populated toward the end of the heating process (Figure 4B) were more compact than for the positive-only scenario (Figure 4A). Throughout the runs, each A^- was in salt bridge contact with at least one BH^+. These salt bridge motifs ranged from simple BH^+/A^- pairs to larger clusters. An example of the latter can be seen in Figure 4B at 1000 K where NT^+/$Glu51^-$/$Lys29^+$/$Asp21^-$/$Lys33^+$ are clustered together.

(3) *Mobile H^+ simulations*[30, 60] allow for H^+ transfer, governed by *PA* values and conformation-dependent electrostatic energies.[30, 60] This type of simulation accounts for H^+ migration that is known to take place in gaseous proteins.[52-56] Protein conformations populated

during heating are depicted in Figure 4C, starting with native-like conformers at 300 K all the way to unfolded structures at 1000 K. Throughout these runs the number of A^- sites fluctuated due to the reversible deprotonation of carboxylates. As discussed earlier (Figures 1, 2B), the viability of zwitterionic motifs depends on the distances and the electrostatic environment of the participating sites. This is reflected in the gradual A^- accumulation early during the runs; the initial (crystal) structure did not yield any salt bridges, whereas side chain reorientation after 30 ns of gas phase equilibration at 300 K yielded 3 ± 1 A^- (Figures 5A, S6C). Similar to Figure 4B, all A^- sites in the mobile H^+ simulations formed salt bridges with at least one BH^+. Unfolded conformers at high temperature were somewhat less conducive to the formation of zwitterionic motifs, because base/acid moieties tended to be separated during CIU (consistent with the predictions of Figure 1). As a result, the number of salt bridges decreased as the temperature approached 1000 K (Figure 5A).

CIU Behavior of the Three MD Models. CIU events can be characterized by tracking the radius of gyration (R_g). For temperatures between 300 K and 400 K all MD runs retained compact structures with $R_g \approx 1.2$ nm. At higher temperatures the three models exhibited markedly different behavior (Figure 5B). Positive-only static H^+ simulations produced the most expanded CIU structures with $R_g \approx 3.2$ nm at 1000 K (blue, Figure 5B). Zwitterionic static H^+ runs remained much more compact, with $R_g \approx 2.4$ nm at 1000 K (red, Figure 5B). This difference reflects the strong BH^+/A^- contacts that favor more compact CIU structures in the zwitterionic model. In contrast, the weak B^0/HA^0 and charge-dipole contacts of the positive-only model (Figure S7) are easily disrupted, favoring more expanded structures. The CIU differences of these two static H^+ models are consistent with our COM pulling simulations, where BH^+/A^- had *DE* values that were roughly one order of magnitude larger than for B^0/HA^0 (first two lines for each base/acid pair in Table 1).

Mobile H^+ runs (black, Figure 5B) produced R_g values intermediate between those of the static models. From this result it can be concluded that salt bridges reduce the extent of CIU compared to all-positive scenarios. This is true even when considering the fact[52-56] that strongly bound BH^+/A^- can convert to weak B^0/HA^0 contacts as the result of mobile H^+ (eq. 1). However, the fleeting nature of salt bridges in the mobile H^+ model renders them less effective stabilizers than for the static H^+ zwitterionic model. The intermediate R_g values of the mobile H^+ simulations are consistent with Table 1, where *DE* values for mobile H^+ salt bridges (third line for each base/acid pair) are between those of the static BH^+/A^- and B^0/HA^0 contacts.

Gas Phase Structures: MD and Experiments. Figure 5C shows Ω values for the three MD models at various stages of heating. Positive-only static H^+ runs produced the largest Ω at 1000 K. Significantly smaller values were seen for the zwitterionic static H^+ runs. The mobile H^+ Ω values were intermediate between those of the two static H^+ models. These trends are consistent with the R_g data of Figure 5B, although the Ω values in Figure 5C show considerable standard deviations that reflect the heterogeneity of the MD structures. There is no straightforward relationship between Ω and other measures of protein "size" (such as R_g),[99] which explains why the profile shapes of Figure 5B do not exactly match those of Figure 5C.

The two horizontal lines in Figure 5C represent experimental Ω maxima for the most gentle and for the harshest conditions. The value measured at CE = 0 V agrees well with the MD-generated 300 K Ω values for all three models. This agreement supports the fidelity of the computational and experimental strategies used in this work.

Comparing Ω values of MD-generated CIU structures with experimental CE = 80 V ions is less straightforward for a number of reasons: (1) From existing data on thermometer ions it is

difficult to determine the effective temperature of highly excited ions in CIU experiments.[100, 101] Moreover, it is unclear how to map experimental ion temperatures to a specific MD temperature.[33] (2) The extent of experimental CIU is limited by the fact that excess heating destroys the ions via CID (see protein fragments at CE = 80 V, Figure 3C). This is in contrast to MD simulations where proteins remain covalently intact at any temperature. (3) The MD time scale (130 ns) is much shorter than the heating time of ions in the trap cell (ms). (4) Collisionally heated proteins may undergo structural changes as they lose internal energy in the ~300 K gas during storage and/or passage through the IMS device.[94] As a result of issues 1-4, it is not clear which of the MD temperature points should be compared to the CE = 80 V experiments. Figure 5C reveals that the CE = 80 V experimental Ω agrees with both the mobile H^+ model and the positive-only static H^+ model for an MD temperature of 650 K. The zwitterionic static H^+ runs yielded a Ω value that was 23% lower than the experimental result at this temperature (Figure 5C).

Overall, the data in Figure 5C suggest that the CE = 80 V experimental conditions are roughly comparable to an MD temperature of 650 K. The MD-generated Ω values in this range only show a small difference between the mobile H^+ model and the positive-only static H^+ runs. A significantly lower Ω was obtained for the zwitterionic model with static H^+. This pattern reiterates that mobile H^+ significantly reduce the stabilizing effects of salt bridges.

Conclusions

An analogy may help illustrate the key question explored in this work. Consider two engine parts that are held together by a nut and a bolt, e.g., in a car. If properly fastened, the nut/bolt system will provide a very stable mechanical connection. Now imagine a scenario where the nut is not properly tightened. The two engine parts will remain connected as long as the nut is in place. However,

mechanical agitation can cause the nut to become undone, such that the connection between the engine parts becomes precariously weak. The "loose nut" in this analogy the mobile H^+ in a salt bridge that can convert a strong BH^+/A^- bond into a weak B^0/HA^0 contact.

The known presence of zwitterionic motifs in gaseous biomolecular ions[30, 31, 45-50] makes it tempting to assume that zwitterionic MD models adequately describe the behavior of electrosprayed ions. However, when neglecting the effects of mobile H^+, zwitterionic models overestimate the extent to which salt bridges stabilize protein structures under CIU conditions. The reason for the limited usefulness of static zwitterionic models is that they retain the initial user-defined charge patterns in perpetuity, not allowing for the fact[52-56] that H^+ migration can change the location of charge sites, along with the formation/ annihilation of zwitterionic motifs. Unfortunately, standard MD force fields that are widely used for gas phase simulations do not allow for mobile H^+.[73, 102] The application of mobile H^+ models, as in the current work and a handful of previous studies,[30, 32, 52, 60] seems an important step toward a more realistic description of gaseous biomolecular ions.

Mobile H^+ models account for the fleeting nature of zwitterionic motifs, providing a description that is more realistic than traditional MD strategies that use static positive-only or static zwitterionic patterns. However, we agree with the opinion recently expressed by some community members[103] that mobile H^+ algorithms of the type used here are still quite simplistic and have to be further refined in the future. Work in this direction is currently ongoing in our laboratory.

Supporting Information

Figures S1-S7: Integration methods for *DE* determination; COM pulling MD simulations for Arg/Glu; COM pulling MD simulations for His/Glu; Ubiquitin CID spectrum; Ubiquitin IMS data

acquired on Synapt G2Si and G2; Ubiquitin protonation patterns; [ubiquitin + 6H]$^{6+}$ H-bonds in positive-only model.

References

(1) Dill, K. A.; MacCallum, J. L. The protein-folding problem, 50 years on. *Science* **2012,** *338*, 1042-1046.
(2) Stadler, A. M.; Koza, M. M.; Fitter, J. Determination of conformational entropy of fully and partially folded conformations of holo- and apomyoglobin. *J. Phys. Chem. B* **2015,** *119*, 72-82.
(3) Kazlauskas, R. Engineering more stable proteins. *Chem. Soc. Rev.* **2018,** *47*, 9026-9045.
(4) Baxa, M. C.; Haddadian, E. J.; Jumper, J. M.; Freed, K. F.; Sosnick, T. R. Loss of conformational entropy in protein folding calculated using realistic ensembles and its implications for nmr-based calculations. *Proc. Natl. Acad. Sci. U.S.A.* **2014,** *111*, 15396-15401.
(5) Brini, E.; Fennell, C. J.; Fernandez-Serra, M.; Hribar-Lee, B.; Luksic, M.; Dill, K. A. How water's properties are encoded in its molecular structure and energies. *Chem. Rev.* **2017,** *117*, 12385-12414.
(6) Fersht, A. R., *Structure and mechanism in protein science*. W. H. Freeman & Co.: New York, 1999.
(7) Hendsch, Z. S.; Tidor, B. Do salt bridges stabilize proteins? A continuum electrostatic analysis. *Protein Sci.* **1994,** *3*, 211-226.
(8) Donald, J. E.; Kulp, D. W.; DeGrado, W. F. Salt bridges: Geometrically specific, designable interactions. *Proteins* **2011,** *79*, 898-915.
(9) Kumar, S.; Nussinov, R. Salt bridge stability in monomeric proteins. *J. Mol. Biol.* **1999,** *293*, 1241-1255.
(10) Bosshard, H. R.; Marti, D. N.; Jelesarov, I. Protein stabilization by salt bridges: Concepts, experimental approaches and clarification of some misunderstandings. *J. Mol. Recognit.* **2004,** *17*, 1-16.
(11) Norouzy, A.; Assaf, K. I.; Zhang, S.; Jacob, M. H.; Nau, W. M. Coulomb repulsion in short polypeptides. *J. Phys. Chem. B* **2015,** *119*, 33-43.
(12) Fenn, J. B. Electrospray wings for molecular elephants (nobel lecture). *Angew. Chem. Int. Ed.* **2003,** *42*, 3871-3894.
(13) Seo, J.; Hoffmann, W.; Warnke, S.; Bowers, M. T.; Pagel, K.; von Helden, G. Retention of native protein structures in the absence of solvent: A coupled ion mobility and spectroscopic study. *Angew. Chem.-Int. Edit.* **2016,** *55*, 14173-14176.
(14) Susa, A. C.; Xia, Z. J.; Williams, E. R. Native mass spectrometry from common buffers with salts that mimic the extracellular environment. *Angew. Chem.-Int. Edit.* **2017,** *56*, 7912-7915.
(15) Mehmood, S.; Allison, T. M.; Robinson, C. V. Mass spectrometry of protein complexes: From origins to applications. *Annu. Rev. Phys. Chem.* **2015,** *66*, 453-474.
(16) Leney, A. C.; Heck, A. J. R. Native mass spectrometry: What is in the name? *J. Am. Soc. Mass Spectrom.* **2017,** *28*, 5-13.
(17) Benesch, J. L. P.; Ruotolo, B. T. Mass spectrometry: Come of age for structural and dynamical biology. *Curr. Op. Struct. Biol.* **2011,** *21*, 641-649.
(18) Sharon, M. How far can we go with structural mass spectrometry of protein complexes? *J. Am. Soc. Mass Spectrom.* **2010,** *21*, 487-500.
(19) Wyttenbach, T.; Bowers, M. T. Structural stability from solution to the gas phase: Native solution structure of ubiquitin survives analysis in a solvent-free ion mobility–mass spectrometry environment. *J. Phys. Chem. B* **2011,** *115*, 12266-12275.
(20) Jurneczko, E.; Barran, P. E. How useful is ion mobility mass spectrometry for structural biology? The relationship between protein crystal structures and their collision cross sections in the gas phase. *Analyst* **2011,** *136*, 20-28.
(21) Eldrid, C.; Ujma, J.; Kalfas, S.; Tomczyk, N.; Giles, K.; Morris, M.; Thalassinos, K. Gas phase stability of protein ions in a cyclic ion mobility spectrometry traveling wave device. *Analytical Chemistry* **2019,** *91*, 7554-7561.
(22) Hendricks, N. G.; Julian, R. R. Leveraging ultraviolet photodissociation and spectroscopy to investigate peptide and protein three-dimensional structure with mass spectrometry. *Analyst* **2016,** *141*, 4534-4540.
(23) Clemmer, D. E.; Russell, D. H.; Williams, E. R. Characterizing the conformationome: Toward a structural understanding of the proteome. *Accounts Chem. Res.* **2017,** *50*, 556-560.
(24) van der Spoel, D.; Marklund, E. G.; Larsson, D. S. D.; Caleman, C. Proteins, lipids, and water in the gas phase. *Macromol. Biosci.* **2011,** *11*, 50-59.
(25) Sever, A. I. M.; Konermann, L. Gas phase protein folding triggered by proton stripping generates inside-out structures: A molecular dynamics simulation study. *J. Phys. Chem. B* **2020,** *124*, 3667-3677.
(26) Chen, S.-H.; Russell, D. H. How closely related are conformations of protein ions sampled by im-ms to native solution structures? *J. Am. Soc. Mass Spectrom.* **2015,** *26*, 1433-1443.
(27) Breuker, K.; McLafferty, F. W. Stepwise evolution of protein native structure with electrospray into the gas phase, 10^{-12} to 10^{2} s. *Proc. Natl. Acad. Sci. U.S.A.* **2008,** *105*, 18145-18152.

(28) Mao, Y.; Woenckhaus, J.; Kolafa, J.; Ratner, M. A.; Jarrold, M. F. Thermal unfolding of unsolvated cytochrome c: Experiment and molecular dynamics simulations. *J. Am. Chem. Soc.* **1999,** *121*, 2712-2721.
(29) Hall, Z.; Politis, A.; Bush, M. F.; Smith, L. J.; Robinson, C. V. Charge-state dependent compaction and dissociation of protein complexes: Insights from ion mobility and molecular dynamics. *J. Am. Chem. Soc.* **2012,** *134*, 3429-3438.
(30) Bakhtiari, M.; Konermann, L. Protein ions generated by native electrospray ionization: Comparison of gas phase, solution, and crystal structures. *J. Phys. Chem. B* **2019,** *123*, 1784-1796.
(31) Gantman, T.; Goldstein, M.; Segev, E.; Gerber, R. B. Conformers of ubiquitin 6+ for different charge distributions: Atomistic structures and ion mobility cross sections. *J. Phys. Chem. B* **2019,** *123*, 6401-6409.
(32) Fegan, S. K.; Thachuk, M. A charge moving algorithm for molecular dynamics simulations of gas-phase proteins. *J. Chem. Theory Comput.* **2013,** *9*, 2531-2539.
(33) Zhang, J. C.; Bogdanov, B.; Parkins, A.; McCallum, C. M. Observation of magic number clusters from thermal dissociation molecular dynamics simulations of lithium formate ionic clusters. *J. Phys. Chem. A* **2020,** *124*, 3535-3541.
(34) Baumketner, A.; Bernstein, S. L.; Wyttenbach, T.; Bitan, G.; Teplow, D. B.; Bowers, M. T.; Shea, J. E. Amyloid β-protein monomer structure: A computational and experimental study. *Protein Sci.* **2006,** *15*, 420-428.
(35) Wolynes, P. G. Biomolecular folding in vacuo!!!(?). *Proc. Natl. Acad. Sci. U.S.A.* **1995,** *92*, 2426-2427.
(36) Robinson, C. V.; Chung, E. W.; Kragelund, B. B.; Knudsen, J.; Aplin, R. T.; Poulsen, F. M.; Dobson, C. M. Probing the nature of noncovalent interactions by mass spectrometry. A study of protein-coa ligand binding and assembly. *J. Am. Chem. Soc.* **1996,** *118*, 8646-8653.
(37) Bich, C.; Baer, S.; Jecklin, M. C.; Zenobi, R. Probing the hydrophobic effect of noncovalent complexes by mass spectrometry. *J. Am. Soc. Mass Spectrom.* **2010,** *21*, 286-289.
(38) Liu, L.; Michelsen, K.; Kitova, E. N.; Schnier, P. D.; Klassen, J. S. Energetics of lipid binding in a hydrophobic protein cavity. *J. Am. Chem. Soc.* **2012,** *134*, 3054-3060.
(39) Breuker, K.; Brüschweiler, S.; Tollinger, M. Electrostatic stabilization of a native protein structure in the gas phase. *Angew. Chem. Int. Ed.* **2011,** *50*, 873-877.
(40) Yin, S.; Loo, J. A. Elucidating the site of protein-atp binding by top-down mass spectrometry. *J. Am. Soc. Mass Spectrom.* **2010,** *21*, 899-907.
(41) Gilbert, J. D.; Prentice, B. M.; McLuckey, S. A. Ion/ion reactions with "onium" reagents: An approach for the gas-phase transfer of organic cations to multiply-charged anions. *J. Am. Soc. Mass Spectrom.* **2015,** *26*, 818-825.
(42) Moser, A.; Range, K.; York, D. M. Accurate proton affinity and gas-phase basicity values for molecules important in biocatalysis. *J. Phys. Chem. B* **2010,** *114*, 13911-13921.
(43) Csaszar, A. G. Conformers of gaseous glycine. *J. Am. Chem. Soc.* **1992,** *114*, 9568-9575.
(44) Schnier, P. D.; Gross, D. S.; Williams, E. R. Electrostatic forces and dielectric polarizability of multiply protonated gas-phase cytochrome c ions probed by ion/molecule chemistry. *J. Am. Chem. Soc.* **1995,** *117*, 6747-6757.
(45) Bonner, J. G.; Lyon, Y. A.; Nellessen, C.; Julian, R. R. Photoelectron transfer dissociation reveals surprising favorability of zwitterionic states in large gaseous peptides and proteins. *J. Am. Chem. Soc.* **2017,** *139*, 10286-10293.
(46) Yoo, H. J.; Wang, N.; Zhuang, S. Y.; Song, H. T.; Hakansson, K. Negative-ion electron capture dissociation: Radical-driven fragmentation of charge-increased gaseous peptide anions. *J. Am. Chem. Soc.* **2011,** *133*, 16790-16793.
(47) Marchese, R.; Grandori, R.; Carloni, P.; Raugei, S. On the zwitterionic nature of gas-phase peptides and protein ions. *PLoS Comput. Biol.* **2010,** *6*, e1000775.
(48) Forbes, M. W.; Bush, M. F.; Polfer, N. C.; Oomens, J.; Dunbar, R. C.; Williams, E. R.; Jockusch, R. A. Infrared spectroscopy of arginine cation complexes: Direct observation of gas-phase zwitterions. *J. Phys. Chem. A* **2007,** *111*, 11759-11770.
(49) Zhang, Z.; Browne, S. J.; Vachet, R. W. Exploring salt bridge structures of gas-phase protein ions using multiple stages of electron transfer and collision induced dissociation. *J. Am. Soc. Mass Spectrom.* **2014,** *25*, 604-613.
(50) Ogorzalek Loo, R. R.; Loo, J. A. Salt bridge rearrangement (sabre) explains the dissociation behavior of noncovalent complexes. *J. Am. Soc. Mass Spectrom.* **2016,** *27*, 975-990.
(51) Popa, V.; Trecroce, D. A.; McAllister, R. G.; Konermann, L. Collision-induced dissociation of electrosprayed protein complexes: An all-atom molecular dynamics model with mobile protons. *J. Phys. Chem. B* **2016,** *120*, 5114-5124.
(52) Li, J. Y.; Lyu, W. P.; Rossetti, G.; Konijnenberg, A.; Natalello, A.; Ippoliti, E.; Orozco, M.; Sobott, F.; Grandori, R.; Carloni, P. Proton dynamics in protein mass spectrometry. *J. Phys. Chem. Lett.* **2017,** *8*, 1105-1112.
(53) Dongré, A. R.; Jones, J. L.; Somogyi, Á.; Wysocki, V. H. Influence of peptide composition, gas-phase basicity, and chemical modification on fragmentation efficiency: Evidence for the mobile proton model. *J. Am. Chem. Soc.* **1996,** *118*, 8365-8374.

(54) Boyd, R. K.; Somogyi, Á. The mobile proton hypothesis in fragmentation of protonated peptides: A perspective. *J. Am. Soc. Mass Spectrom.* **2010,** *21*, 1275-1278.
(55) Polasky, D. A.; Dixit, S. M.; Keating, M. F.; Gadkari, V. V.; Andrews, P. C.; Ruotolo, B. T. Pervasive charge solvation permeates native-like protein ions and dramatically influences top-down sequencing data. *J. Am. Chem. Soc.* **2020,** *142*, 6750-6760.
(56) Felitsyn, N.; Kitova, E. N.; Klassen, J. S. Thermal decomposition of a gaseous multiprotein complex studied by blackbody infrared radiative dissociation. Investigating the origin of the asymmetric dissociation behavior. *Anal. Chem.* **2001,** *73*, 4647-4661.
(57) Julian, R. R.; Hodyss, R.; Kinnear, B.; Jarrold, M. F.; Beauchamp, J. L. Nanocrystalline aggregation of serine detected by electrospray ionization mass spectrometry: Origin of the stable homochiral gas-phase serine octamer. *J. Phys. Chem. B* **2002,** *106*, 1219-1228.
(58) Warnke, S.; von Helden, G.; Pagel, K. Protein structure in the gas phase: The influence of side-chain microsolvation. *J. Am. Chem. Soc.* **2013,** *135*, 1177-1180.
(59) Schnier, P. D.; Price, W. D.; Jockusch, R. A.; Williams, E. R. Blackbody infrared radiative dissociation of bradykinin and its analogues: Energetics, dynamics, and evidence for salt-bridge structures in the gas phase. *J. Am. Chem. Soc.* **1996,** *118*, 7178-7189.
(60) Konermann, L. Molecular dynamics simulations on gas-phase proteins with mobile protons: Inclusion of all-atom charge solvation. *J. Phys. Chem. B* **2017,** *121*, 8102-8112.
(61) Nouchikian, L.; Lento, C.; Donovan, K. A.; Dobson, R. C.; Wilson, D. J. Comparing the conformational stability of pyruvate kinase in the gas phase and in solution. *Journal of the American Society for Mass Spectrometry* **2020,** *31*, 685-692.
(62) Chan, D. S. H.; Kavanagh, M. E.; McLean, K. J.; Munro, A. W.; Matak-Vinkovic, D.; Coyne, A. G.; Abell, C. Effect of dmso on protein structure and interactions assessed by collision-induced dissociation and unfolding. *Anal. Chem.* **2017,** *89*, 9976-9983.
(63) Pacholarz, K. J.; Barran, P. E. Distinguishing loss of structure from subunit dissociation for protein complexes with variable temperature ion mobility mass spectrometry. *Anal. Chem.* **2015,** *87*, 6271-6279.
(64) Allison, T. M.; Reading, E.; Liko, I.; Baldwin, A. J.; Laganowsky, A.; Robinson, C. V. Quantifying the stabilizing effects of protein-ligand interactions in the gas phase. *Nat. Commun.* **2015,** *6*.
(65) Hopper, J. T. S.; Oldham, N. J. Collision induced unfolding of protein ions in the gas phase studied by ion mobility-mass spectrometry: The effect of ligand binding on conformational stability. *J. Am. Soc. Mass Spectrom.* **2009,** *20*, 1851-1858.
(66) Han, L.; Hyung, S.-J.; Ruotolo, B. T. Bound cations significantly stabilize the structure of multiprotein complexes in the gas phase. *Angew. Chem. Int. Ed.* **2012,** *51*, 5692-5695.
(67) Zheng, X. Y.; Kurulugama, R. T.; Laganowsky, A.; Russell, D. H. Collision-induced unfolding studies of proteins and protein complexes using drift tube ion mobility-mass spectrometer. *Anal. Chem.* **2020,** *92*, 7218-7225.
(68) Benesch, J. L. P. Collisional activation of protein complexes: Picking up the pieces. *J. Am. Soc. Mass Spectrom.* **2009,** *20*, 341-348.
(69) Carvalho, V. V.; See Kit, M. C.; Webb, I. K. Ion mobility and gas-phase covalent labeling study of the structure and reactivity of gaseous ubiquitin ions electrosprayed from aqueous and denaturing solutions. *J. Am. Soc. Mass Spectrom.* **2020,** *31*, 1037-1046.
(70) Shi, H.; Atlasevich , N.; Merenbloom, S. I.; Clemmer, D. E. Solution dependence of the collisional activation of ubiquitin [m + 7h]7+ ions. *J. Am. Soc. Mass Spectrom.* **2014,** *25*, 2000-2008.
(71) Sun, Y.; Vahidi, S.; Sowole, M. A.; Konermann, L. Protein structural studies by traveling wave ion mobility spectrometry: A critical look at electrospray sources and calibration issues. *J. Am. Soc. Mass Spectrom.* **2016,** *27*, 31-40.
(72) Abraham, M. J.; Murtola, T.; Schulz, R.; Páll, S.; Smith, J. C.; Hess, B.; Lindahl, E. Gromacs: High performance molecular simulations through multi-level parallelism from laptops to supercomputers. *SoftwareX* **2015,** *1–2*, 19-25.
(73) Kaminski, G. A.; Friesner, R. A.; Tirado-Rives, J.; Jorgensen, W. L. Evaluation and reparametrization of the opls-aa force field for proteins via comparison with accurate quantum chemical calculations on peptides. *J. Phys. Chem. B* **2001,** *105*, 6474-6487.
(74) Fegan, S. K.; Thachuk, M. Suitability of the martini force field for use with gas-phase protein complexes. *J. Chem. Theory Comput.* **2012,** *8*, 1304-1313.
(75) Marchese, R.; Grandori, R.; Carloni, R.; Raugei, S. A computational model for protein ionization by electrospray based on gas-phase basicity. *J. Am. Soc. Mass Spectrom.* **2012,** *23*, 1903-1910.
(76) Patriksson, A.; Adams, C. M.; Kjeldsen, F.; Zubarev, R. A.; van der Spoel, D. A direct comparison of protein structure in the gas and solution phase: The trp-cage. *J. Phys. Chem. B* **2007,** *111*, 13147-13150.

(77) Hoover, W. G. Canonical dynamics: Equilibrium phase-space distributions. *Phys. Rev. A* **1985,** *31*, 1695-1697.
(78) Jorgensen, W. L.; Maxwell, D. S.; TiradoRives, J. Development and testing of the opls all-atom force field on conformational energetics and properties of organic liquids. *J. Am. Chem. Soc.* **1996,** *118*, 11225-11236.
(79) Goyal, P.; Qian, H. J.; Irle, S.; Lu, X. Y.; Roston, D.; Mori, T.; Elstner, M.; Cui, Q. Molecular simulation of water and hydration effects in different environments: Challenges and developments for dftb based models. *J. Phys. Chem. B* **2014,** *118*, 11007-11027.
(80) Barnes, G. L.; Hase, W. L. Energy transfer, unfolding, and fragmentation dynamics in collisions of n-protonated octaglycine with an h-sam surface. *J. Am. Chem. Soc.* **2009,** *131*, 17185-17193.
(81) Marx, D.; Chandra, A.; Tuckerman, M. E. Aqueous basic solutions: Hydroxide solvation, structural diffusion, and comparison to the hydrated proton. *Chem. Rev.* **2010,** *110*, 2174-2216.
(82) Iyengar, S. S.; Day, T. J. F.; Voth, G. A. On the amphiphilic behavior of the hydrated proton: An ab initio molecular dynamics study. *Int. J. Mass Spectrom.* **2005,** *241*, 197-204.
(83) Burlet, O.; Orkiszewski, R. S.; Ballard, K. D.; Gaskell, S. J. Charge promotion of low-energy fragmentations of peptide ions. *Rapid Commun. Mass Spectrom.* **1992,** *6*, 658-662.
(84) Cautereels, J.; Blockhuys, F. Quantum chemical mass spectrometry: Verification and extension of the mobile proton model for histidine. *J. Am. Soc. Mass Spectrom.* **2017,** *28*, 1227-1235.
(85) Nakai, H.; Sakti, A. W.; Nishimura, Y. Divide-and-conquer-type density-functional tight-binding molecular dynamics simulations of proton diffusion in a bulk water system. *J. Phys. Chem. B* **2016,** *120*, 217-221.
(86) Sudmeier, J. L.; Bradshaw, E. M.; Haddad, K. E. C.; Day, R. M.; Thalhauser, C. J.; Bullock, P. A.; Bachovchin, W. W. Identification of histidine tautomers in proteins by 2d h-1/c-13(delta 2) one-bond correlated nmr. *J. Am. Chem. Soc.* **2003,** *125*, 8430-8431.
(87) Ewing, S. A.; Donor, M. T.; Wilson, J. W.; Prell, J. S. Collidoscope: An improved tool for computing collisional cross-sections with the trajectory method. *J. Am. Soc. Mass Spectrom.* **2017,** *28*, 587-596.
(88) Isralewitz, B.; Gao, M.; Schulten, K. Steered molecular dynamics and mechanical functions of proteins. *Curr. Opin. Struct. Biol.* **2001,** *11*, 224-230.
(89) Pu, J.; Karplus, M. How subunit coupling produces the γ-subunit rotary motion in f_1-atpase. *Proc. Natl. Acad. Sci. U.S.A.* **2008,** *105*, 1192-1197.
(90) Schonfelder, J.; Perez-Jimenez, R.; Munoz, V. A simple two-state protein unfolds mechanically via multiple heterogeneous pathways at single-molecule resolution. *Nat. Commun.* **2016,** *7*.
(91) Lemkul, J. A.; Bevan, D. R. Assessing the stability of alzheimer's amyloid protofibrils using molecular dynamics. *J. Phys. Chem. B* **2010,** *114*, 1652-1660.
(92) Paizs, B.; Suhai, S. Fragmentation pathways of protonated peptides. *Mass Spectrom. Rev.* **2005,** *24*, 508-548.
(93) Donor, M. T.; Mroz, A.; Prell, J. S. Experimental and theoretical investigation of overall energy deposition in surface-induced unfolding of protein ions. *Chem. Sci.* **2019,** *10*, 4097-4106.
(94) Giles, K.; Williams, J. P.; Campuzano, I. Enhancements in travelling wave ion mobility resolution. *Rapid Commun. Mass Spectrom.* **2011,** *25*, 1559-1566.
(95) Valentine, S. J.; Counterman, A. E.; Clemmer, D. E. Conformer-dependent proton-transfer reactions of ubiquitin ions. *J. Am. Soc. Mass Spectrom.* **1997,** *8*, 954-961.
(96) Klassen, J. S.; Kebarle, P. Collision-induced dissociation threshold energies of protonated glycine, glycinamide, and some related small peptides and peptide amino amides. *J. Am. Chem. Soc.* **1997,** *119*, 6552-6563.
(97) Shelimov, K. B.; Jarrold, M. F. Conformations, unfolding, and refolding of apomyoglobin in vacuum: An activation barrier for gas-phase protein folding. *J. Am. Chem. Soc.* **1997,** *119*, 2987-2994.
(98) Steinberg, M. Z.; Elber, R.; McLafferty, F. W.; Gerber, R. B.; Breuker, K. Early structural evolution of native cytochrome c after solvent removal. *ChemBioChem* **2008,** *9*, 2417-2423.
(99) Hewitt, D.; Marklund, E.; Scott, D. J.; Robinson, C. V.; Borysik, A. J. A hydrodynamic comparison of solution and gas phase proteins and their complexes. *J. Phys. Chem. B* **2014,** *118*, 8489-8495.
(100) Ieritano, C.; Featherstone, J.; Haack, A.; Guna, M.; Campbell, J. L.; Hopkins, W. S. How hot are your ions in differential mobility spectrometry? *Journal of the American Society for Mass Spectrometry* **2020,** *31*, 582-593.
(101) Merenbloom, S. I.; Flick, T. G.; Williams, E. R. How hot are your ions in twave ion mobility spectrometry? *J. Am. Soc. Mass Spectrom.* **2012,** *23*, 553-562.
(102) Huang, J.; MacKerell, A. D. Charmm36 all-atom additive protein force field: Validation based on comparison to nmr data. *J. Comput. Chem.* **2013,** *34*, 2135-2145.
(103) Allison, T. M.; Barran, P.; Cianferani, S.; Degiacomi, M. T.; Gabelica, V.; Grandori, R.; Marklund, E. G.; Menneteau, T.; Migas, L. G.; Politis, A., et al. Computational strategies and challenges for using native ion mobility mass spectrometry in biophysics and structural biology. *Anal. Chem.* **2020,** *92*, 10872-10880.

Table 1. Gas phase dissociation energies (*DE*, in kJ mol^{-1}) of salt brige vs. neutral base/acid side chain contacts. Data were generated for peptide 1 (Gly-**Base**-Ala, where Base = Lys or Arg or His) and peptide 2 (Ala-**Glu**-Gly). Raw data are illustrated in Figures 2 and S1-S3. The initial two lines for each base/acid pair are for static protonation patterns; H^+ migration is only considered for the third entries. Two possible tautomers were considered for neutral His (HisD and HisE) which have a Nε-H or Nδ-H group, respectively.[86]

Lys/Glu	salt bridge	neutral
uncorrected eq. 3 value (static H^+)	1070 ± 10	86 ± 4
after correction for secondary H-bonds (static H^+)	880 ± 10	40 ± 10
after addtl. correction for mobile H^+	200 ± 100	n/a

Arg/Glu	salt bridge	neutral
uncorrected eq. 3 value (static H^+)	940 ± 30	100 ± 20
after correction for secondary H-bonds (static H^+)	720 ± 20	60 ± 10
after addtl. correction for mobile H^+	600 ± 100	n/a

His/Glu	salt bridge	neutral (HisD)	neutral (HisE)
uncorrected eq. 3 value (static H^+)	920 ± 60	100 ± 10	90 ± 10
after correction for secondary H-bonds (static H^+)	600 ± 20	30 ± 10	20 ± 10
after addtl. correction for mobile H^+	300 ± 200	n/a	n/a

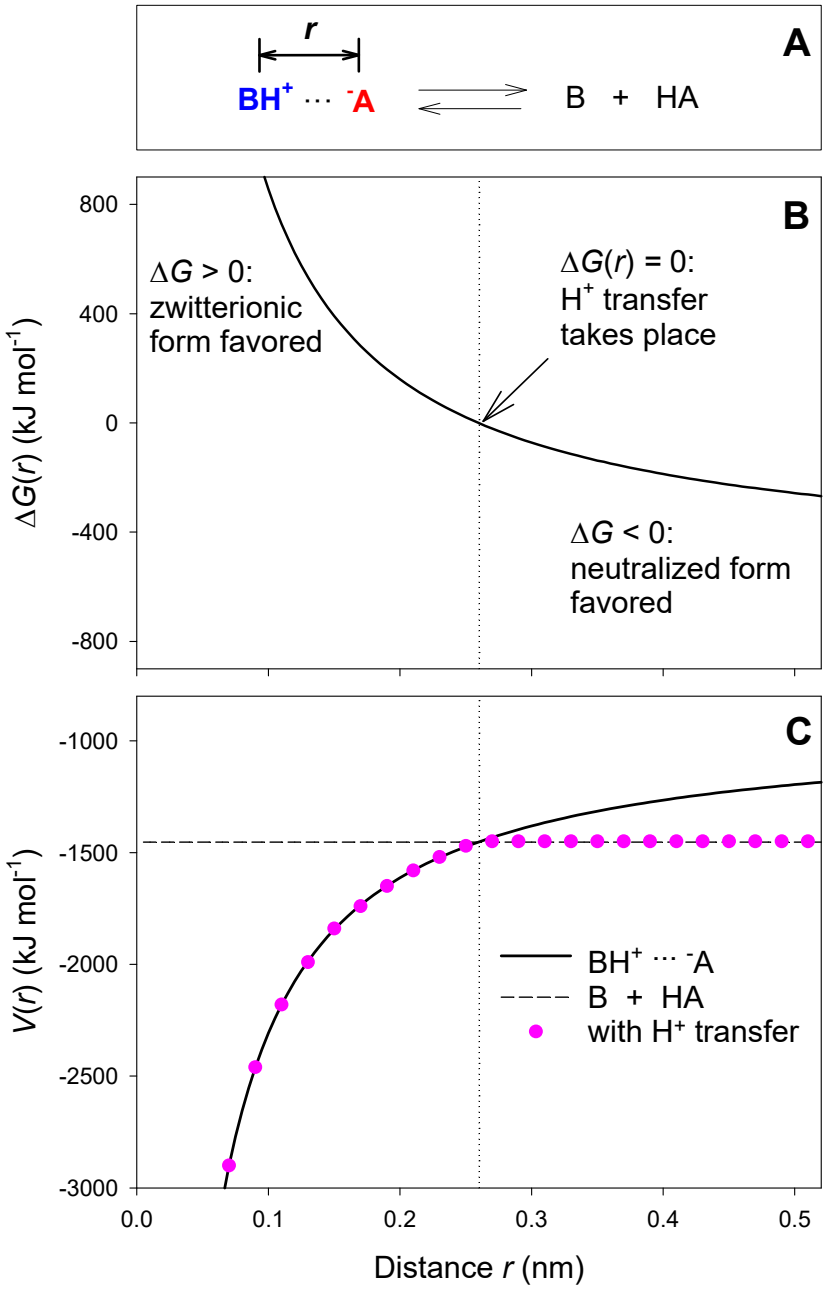

Figure 1. (A) Simple point charge model that qualitatively illustrates the behavior of a basic/acidic side chain pair in the gas phase. The residues can either be zwitterionic and form a salt bridge (left), or they can form a neutralized pair (right). (B) Free energy ΔG of the neutralization reaction, calculated as a function of distance r using eq. 2 with $PA(A^-)$ = 1453 kJ mol^{-1} (Asp^-) and PA(B) = 918 kJ mol^{-1} (Lys).[42] The neutralized pair is favored for large r, implying that H^+ transfer will take place as r increases. (C) Potential energy profiles $V(r)$ of the zwitterionic form and the neutralized form. H^+ transfer causes the system to cross over from one profile to the other, indicated by the magenta dots. Note: The mobile H^+ MD simulations discussed later employed a more sophisticated strategy that also considers H-bonding, intramolecular charge solvation, and Lennard-Jones interactions.

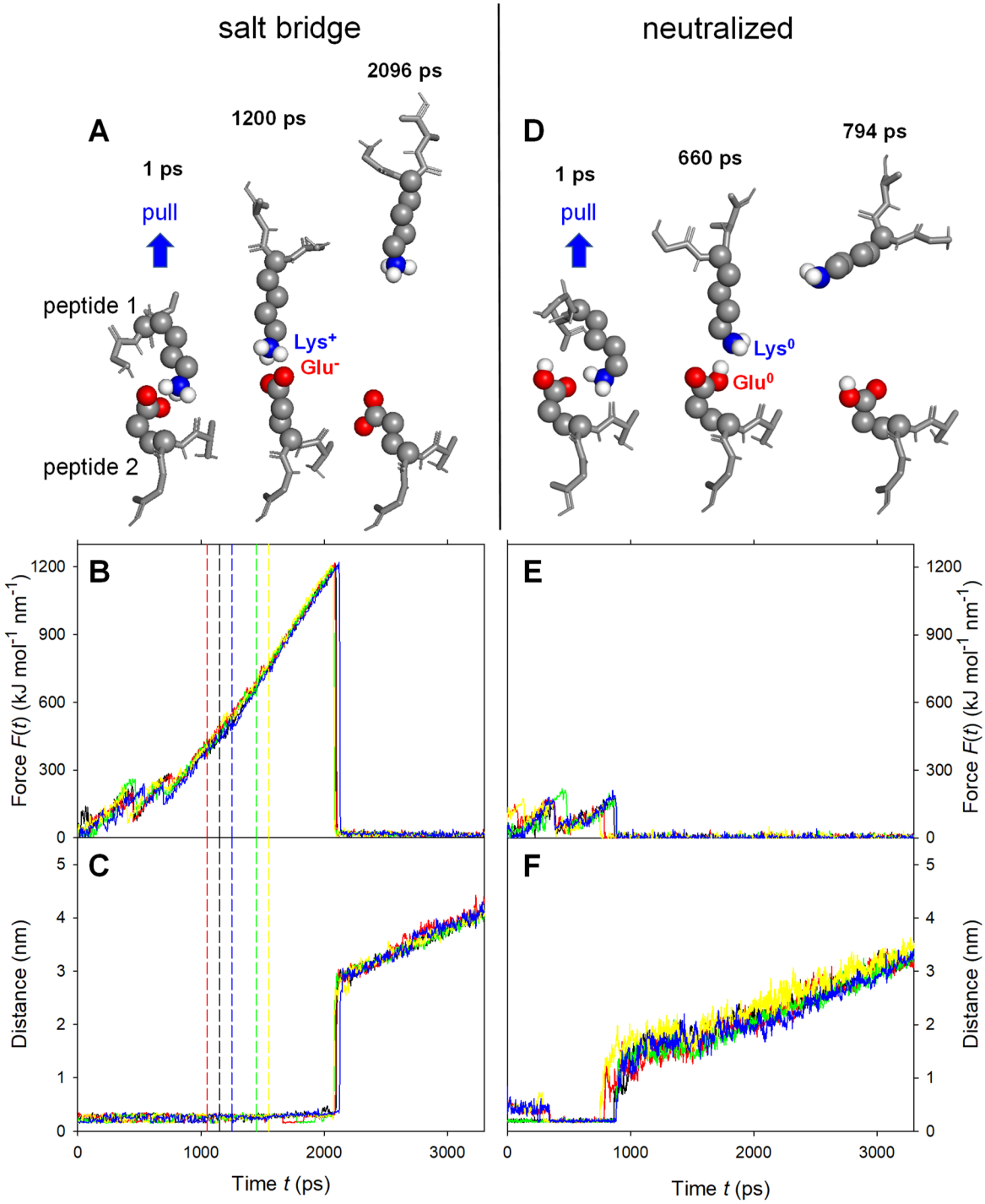

Figure 2. MD pulling results for peptide 1 (Gly-**Lys**-Ala) and peptide 2 (Ala-**Glu**-Gly) in the gas phase. The Lys/Glu side chains are engaged in noncovalent contacts. Peptide 1 is being pulled, peptide 2 is immobilized. (A-C) Salt-bridged Lys^{+}/Glu^{-} scenario. (D-F) Neutralized Lys^{0}/Glu^{0} scenario. Panels A/D: Representative MD snapshots, with Lys/Glu shown as spheres. Panels B/E: Pulling force $F(t)$. Panel C: Distance of the closest Lys-H O-Glu contact vs. time. Panel F: Distance of the Lys-N H-Glu contact vs. time. Time profiles show overlays of five independent runs for each condition. Vertical lines in B/C indicates where Lys^{+}/Glu^{-} would convert to Lys^{0}/Glu^{0} (although this H^{+} transfer event was *not* allowed to take place for the runs in this figure).

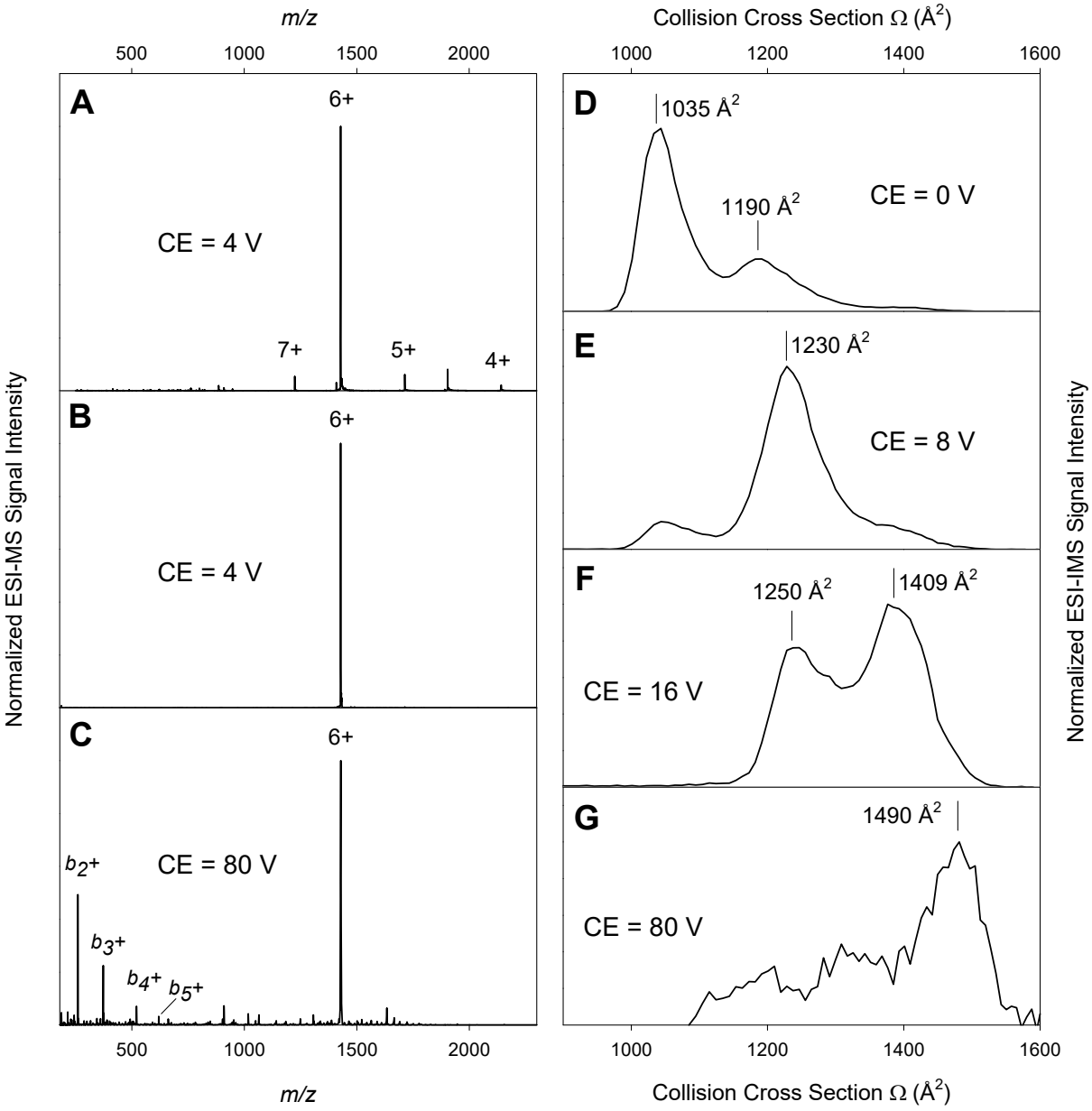

Figure 3. ESI-MS and collision-induced unfolding of [ubiquitin + 6H]$^{6+}$ on a Synapt G2Si instrument. The trap collision energy ("CE") that controls the extent of collisional heating is indicated in each panel. (A) Native ESI mass spectrum. (B) Same as in panel A, but after quadrupole selection of the 6+ charge state. (C) Same as in panel B, but with extensive collisional activation that starts to rupture covalent bonds. Some CID products are annotated (fragment ion identification was performed using the UCSF Protein Prospector; see Figure S4 for additional details). (D-G) Collision cross section distributions at different collision energies.

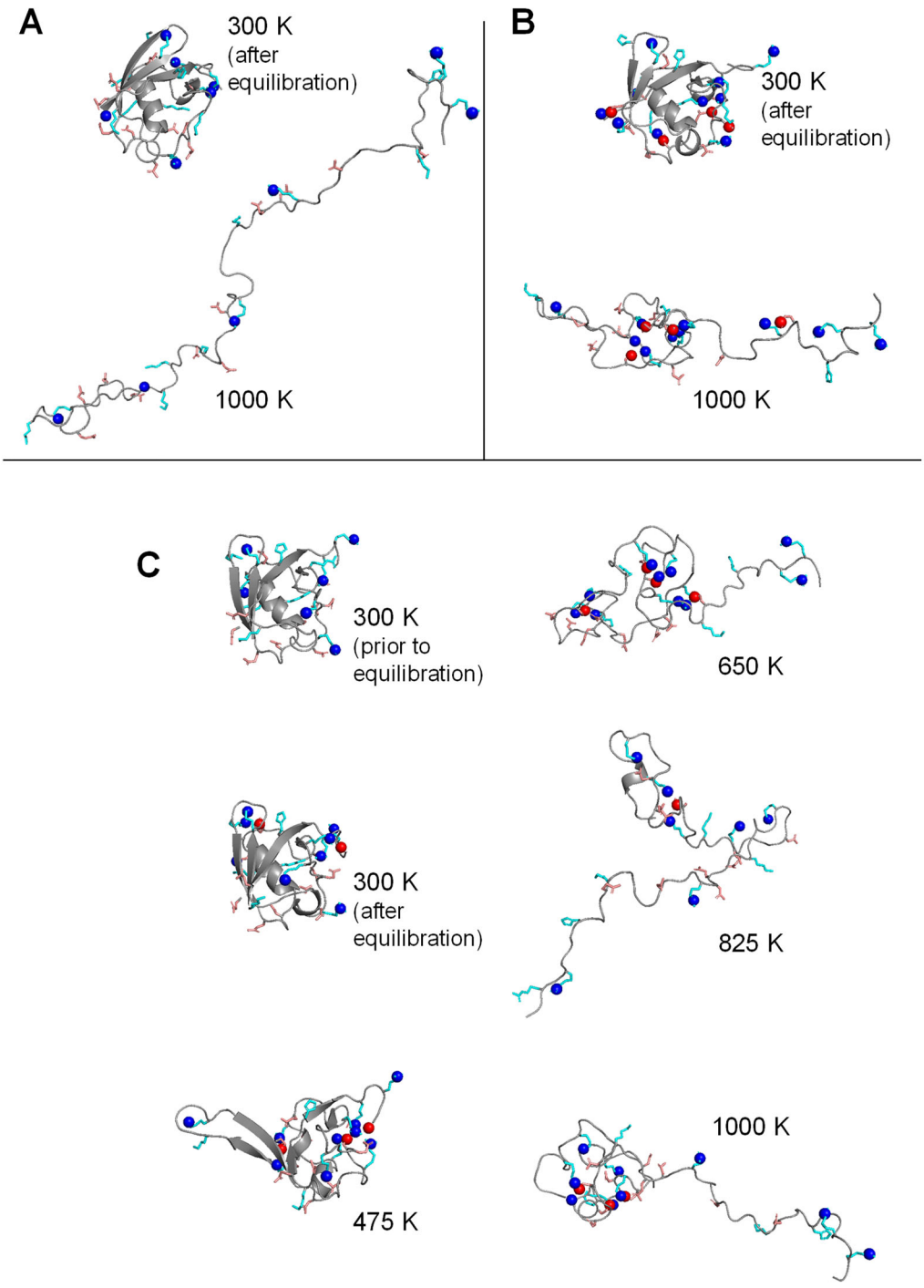

Figure 4. Snapshots taken from MD trajectories during heating of gaseous [ubiquitin + 6H]$^{6+}$. The protein ions were equilibrated at 300 K for 30 ns, followed by gradual heating to 1000 K over 100 ns. (A) Positive-only scenario with static H^+. (B) Zwitterionic scenario with static H^+. (C) MD simulation with mobile H^+. Titratable side chains are shown as sticks; Arg/Lys/His in cyan and Glu/Asp in pale red. Blue and red spheres represent BH^+ and A^- sites, respectively.

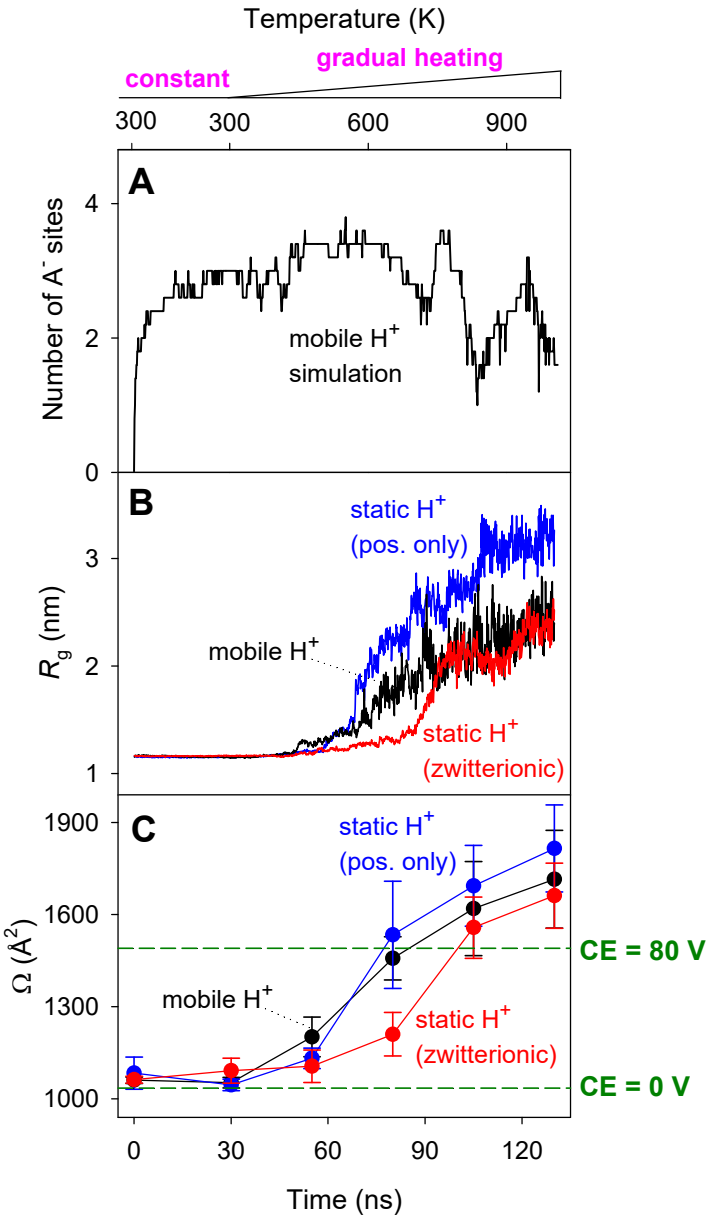

Figure 5. MD results for heating of [ubiquitin + 6H]$^{6+}$ in the gas phase. The temperature profile for these CIU simulations is indicated along the top, i.e., 30 ns of equilibration at 300 K, followed by 100 ns of gradual heating up to 1000 K. (A) Number of negative charges (A^- sites) in mobile H^+ simulations. (B) Radius of gyration (R_g) for runs conducted under different conditions: static H^+ (positive-only), static H^+ (zwitterionic), and with mobile H^+. (C) Ω values of the MD-generated structures. Dashed lines indicate experimental Ω values. All MD profiles are averages of five independent simulations for each condition; error bars represent standard deviations.

TOC Graphic

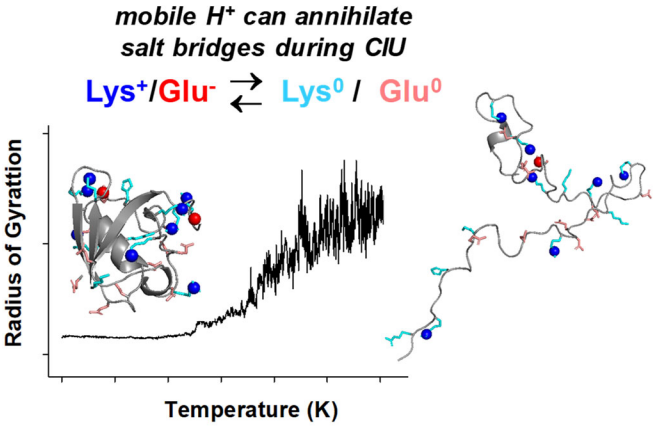
mobile H+ can annihilate
salt bridges during ClU
Lys+/Glu- ⇄ Lys0 / Glu0
Radius of Gyrattion
Temperature (K)